

Location of Achromatizing Pupil Position and First Purkinje Reflection in a Normal Population

Silvestre Manzanera, Pedro M. Prieto, Antonio Benito, Juan Tabernero, and Pablo Artal

Laboratorio de Óptica, Instituto Universitario de Investigación en Óptica y Nanofísica, Universidad de Murcia, Campus de Espinardo (Edificio 34), Murcia, Spain

Correspondence: Pablo Artal, Laboratorio de Óptica, Universidad de Murcia (LO-UM), Instituto Universitario de investigación en Óptica y Nanofísica (IUIOyN), Campus de Espinardo (Edificio 34), 30100 Murcia, Spain; pablo@um.es.

Submitted: November 20, 2014
Accepted: January 7, 2015

Citation: Manzanera S, Prieto PM, Benito A, Tabernero J, Artal P. Location of achromatizing pupil position and first Purkinje reflection in a normal population. *Invest Ophthalmol Vis Sci.* 2015;56:962-966. DOI:10.1167/iov.14-16108

PURPOSE. Quality of vision in patients who have undergone corneal refractive surgery depends upon the optimal centration of the procedures used. The center of the pupil is used as a reference point in some corneal ablation procedures. The achromatic axis would be a more sensible option from an optical point of view, but it is not as readily detectable. As an alternative, other refractive techniques, like the small aperture corneal inlay for presbyopia correction, use the corneal reflex (first Purkinje image). To assess the relative position of these two marks, we developed a new instrument to simultaneously measure both the first Purkinje image (PI) and the intersection of the achromatic axis with the pupil plane.

METHODS. The apparatus records images of the pupil and the PI when illuminated with a circle of infrared light-emitting diodes. A second optical path allows determination of the achromatic axis by using a subjective method. Both the positions of the PI and the achromatic axis intersection are determined simultaneously.

RESULTS. A series of data were obtained in 48 eyes. The mean location of the achromatic point relative to the PI was [$x = -0.05 \pm 0.15$ mm; $y = 0.09 \pm 0.18$ mm]. Considered individually, in 55% of eyes, the distance between locations is less than 0.2 mm, and in 95% of eyes, distances are less than 0.4 mm.

CONCLUSIONS. On average, achromatic axis crossing of the pupil and PI locations coincides within measurement errors. Although there was some intersubject variability, differences in location were less than 0.6 mm in all measured eyes.

Keywords: achromatic axis, centration, corneal inlay, presbyopia, Purkinje images, small aperture

A number of refractive surgical techniques are available for the correction of refractive errors.¹⁻³ Presbyopia also can be partially compensated with approaches such as the small aperture corneal inlay.⁴ Because the human eye is not an aligned, rotationally symmetrical optical system, the question about the optimum location of the treatment's centration of the surgery on the cornea is still open and remains a topic for discussion.

Uozato and Guyton⁵ claimed that the best location for corneal surgery is the center of the entrance pupil instead of the visual axis. Conversely, Pande and Hillman⁶ suggested that the coaxially sighted corneal reflex should be used as the reference point for centration because, in practical terms, it is the easiest way to center on or about the visual axis. It has been shown that this discussion is especially relevant for those eyes with a large angle kappa, which occurs mainly for hyperopic patients.⁷⁻⁹ To clarify our terminology, the visual axis is the line connecting the fovea with the fixation point passing through the nodal point, and the corneal reflex is the virtual image formed by reflection on the first surface of the cornea, also called the first Purkinje image (PI).

A surgical technique that is especially sensitive to centration is the small aperture corneal inlay. It is a theoretically simple concept that can provide good visual acuity for both far and near vision when implanted as a modified monovision approach.¹⁰ The inlay is a small opaque disk with a 1.6-mm

inner aperture to extend depth of focus. However, even a small aperture can produce undesired optical effects if centration is not correct. Displacing a pinhole aperture in front of the eye induces foveal transverse chromatic aberration (TCA), degrading retinal image quality.¹¹⁻¹³ In order to minimize the impact of TCA, the aperture should be located at the intersection of the visual axis with the cornea because in that case, the achromatic axis¹¹ becomes the visual axis and the aperture is at the achromatizing pupil (AcP) position. Tabernero and Artal¹⁴ showed by using numerical simulations with data from real eyes that a decentration of 0.4 mm from a previously estimated optimal point could noticeably decrease image quality. In clinical practice, it is not easy to find the visual axis, but it is assumed, based on model eyes, that for the most part of the population, it lies somewhere between the pupil's center and the corneal reflex, both of which are easily detectable. The typical centration of the corneal inlay is on the corneal vertex, approximately half way between both locations.¹⁵⁻¹⁷

For any of the surgical techniques mentioned above, it is relevant to know the potential mismatch when actually centering on the PI but ideally aiming for the intersection of the visual axis with the cornea. The goal of this work was to determine the location of both reference points and their relative distances in a normal population in order to assess the validity of a widely used procedure for corneal surgery centration. To this end, we designed and built a new

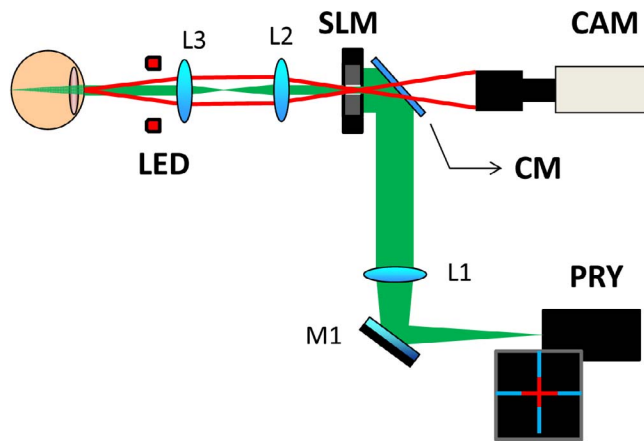


FIGURE 1. Schematic layout of the instrument. A pico-projector (PRY) produces a two-color stimulus that is seen through the small aperture created by the spatial light modulator (SLM). The corneal reflex produced by a semicircular array of LEDs is recorded by means of a camera (CAM) with a telecentric objective through a cold mirror (CM).

instrument capable of simultaneously locating the position of both the corneal reflex and the intersection of the visual axis with the eye pupil plane.

METHODS

We obtained data for 90 eyes from 48 normal subjects (19 males and 29 females). Mean patient age was 29 ± 10 years old (range, 21–59 years of age), and the average axial length was 23.74 ± 1.13 mm (range, 21.94–27.53 mm). On average, our population was slightly myopic, with a mean equivalent refractive error of -0.84 ± 1.42 diopters (D; range, -3.88 to $+1.75$ D). Astigmatism was below 2.5 D for all subjects. Mean pupil diameter was 5.5 ± 1.0 mm (range, 3.4–7.2 mm).

The instrument is able to simultaneously register the positions of both the PI and AcP over the pupil plane. The system was designed with 2 coaligned light paths, 1 to capture an image of the real pupil of the subject (optical path) and the other path to present the eye with a visual chromatic test (visual path).

Figure 1 shows a schematic diagram of the setup. In the optical path (Fig. 1, red lines), the eye is illuminated with a circular array (4-cm diameter) of infrared light-emitting diodes (LEDs; mean $\lambda = 850$ nm) located 5 cm from the subject's pupil plane. This pupil plane is optically conjugated with a transmissive spatial light modulator (SLM) for intensity modulation (model LC2002; Holoeye Photonics AG, Berlin, Germany) using the telescope formed with lenses L2 and L3 (both achromatic doublets of 60-mm focal length). A real-time sequence of images of the pupil plane that also contains the corneal reflection of the circular infrared source (i.e., the PI) is recorded by a complementary metal oxide semiconductor camera sensor (model PL-B741; pixelLINK, Ottawa, ON, Canada) equipped with a telecentric teleobjective lens (0.5 \times ; working distance: 110 mm).

The visual path (Fig. 1, green lines) consists of a pico projector (PRY; Micro professional projector model MPro150; 3M Projection Systems, St. Paul, MN, USA) for generation of the chromatic visual test; a collimating lens (L1; achromatic doublet of 200-mm focal length); and a cold mirror to direct the chromatic test toward the eye coaxially to the optical path. The projector is mounted over a linear stage that allows axial

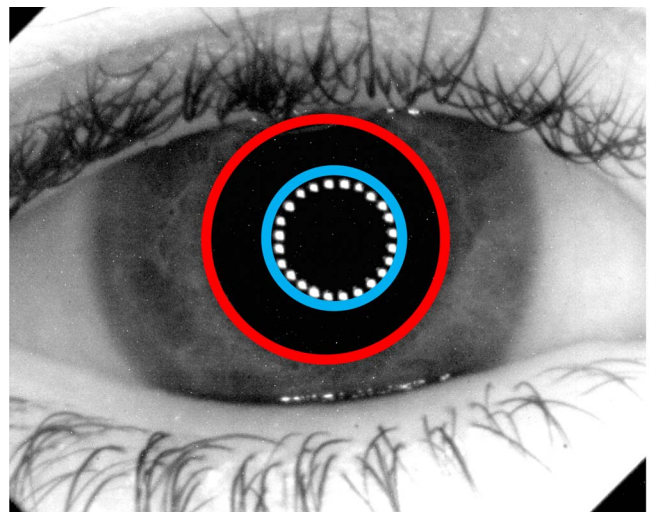


FIGURE 2. Pupil plane picture for one subject. This image was processed to determine the contour (and center) of the pupil (red line) and the corneal reflection circle (blue line). Additionally, the position of the small pupil at the time is also recorded.

displacement to compensate for possible defocus refractive errors (up to ± 4 D). Subjects observe the visual test through a pupil of 1.0 mm diameter generated at the SLM plane. To stabilize the subject's head, a disposable sterile wood tongue depressor was used as a bite bar. This renders the instrument more accurate than when a chin rest is used, and the procedure is simpler and more comfortable for the subject than undergoing a dental impression procedure.

The visual chromatic test consists of a simultaneous X/Y two-color Vernier alignment test similar to that used by Rynders et al.¹⁸ to measure transverse chromatic aberration. An inner cross in red (central $\lambda = 628$ nm) aligned with an outer one in blue (central $\lambda = 456$ nm) are presented to the subject. Angular sizes were 0.34° for the red and 1.15° for the blue crosses respectively.

The experimental procedure started with the alignment of the eye's pupil to the optical axis of the instrument by using real-time images provided by the camera in the optical path. The subject was then instructed to fixate on the chromatic stimulus and move the projector over the linear stage until both crosses were perceived in focus. In theory, this is not achievable due to the longitudinal chromatic aberration and the requirement for the subject was to search for a compromise position that would allow a later proper alignment of the red and blue stimulus. Only when the small aperture is located at the AcP position would the subject see the red and blue crosses properly aligned. Otherwise, some misalignment would be perceived due to the induced TCA. Therefore, the subject's task was to realign both crosses horizontally and vertically by moving in 32- μ m steps the 1.0-mm pupil on the SLM, using the arrow keys of a keyboard. Once both crosses were perceived to be aligned, the subject had to steadily fixate on the crosses and simultaneously press the space bar in the keyboard, triggering the software to save both the small aperture position and an image of the actual pupil and corneal reflection. This procedure was repeated 10 times per each eye. The image recorded was later processed to obtain the center of the eye's pupil and the position of the PI. Figure 2 shows an example of an image recorded and analyzed to estimate the center of the pupil (Fig. 2, red line) and the position of the corneal reflection (Fig. 2, blue line).

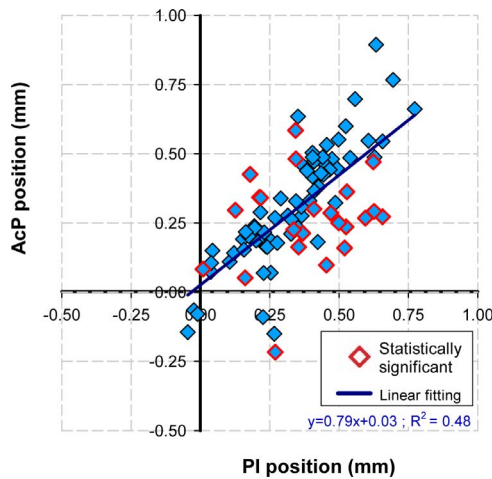


FIGURE 3. Location of PI versus AcP along the horizontal direction (x). The origin of coordinates is the center of the pupil for each eye. Each value corresponds to the mean value across measurements for each subject. The symbols with red outlines correspond to those eyes whose PI and AcP position difference are statistically significant ($P < 0.05$).

RESULTS

Estimates of the AcP and first PI were compared for both the X, horizontal, direction (temporal-nasal) and the Y, vertical, direction (inferior-superior). Positive X or Y values indicated nasal or superior displacement, respectively. The average error in the estimation of the AcP position was 0.17 mm and 0.18 for the X and Y components, respectively, with a maximum uncertainty found in one eye of 0.42 mm and a minimum of 0.04 mm. The variability in determination of PI location is appreciably lower than that for the AcP, with a mean error of 0.03 mm for both components.

Taking the origin of coordinates at the pupil center, the X and Y components of the mean AcP position versus the same component of the PI for each eye are represented in Figures 3 and 4. There was a good linear correlation for the horizontal values ($R^2 = 0.48$) but not for the vertical ones ($R^2 = 0.09$).

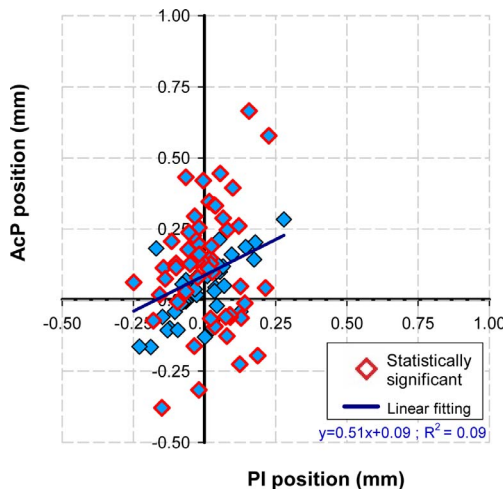


FIGURE 4. Location of PI versus AcP along the vertical direction (y). The origin of coordinates is the center of the pupil for each eye. Each value corresponds to the mean value across measurements for each subject. Symbols with red outlines correspond to those eyes whose PI and AcP positions are statistically significant ($P < 0.05$).

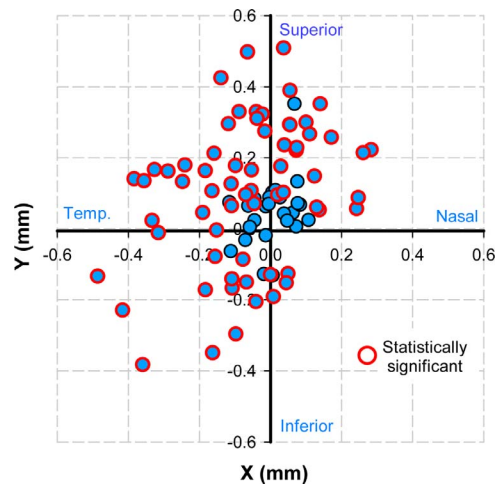


FIGURE 5. AcP positions relative to those of PI. Those eyes where distances between AcP and PI were found to be statistically significant ($P < 0.05$) are shown with a red outline.

We determined the number of eyes where the AcP and PI locations were not coincident considering the experimental uncertainty in the determination of both locations. A statistical analysis using a Student's *t*-test (two-sided, different variance) was carried out over the set of estimations in the positions of AcP and PI for each subject. Those eyes where the differences between these locations were statistically significant ($P < 0.05$) in X or Y direction are highlighted in Figures 3 and 4, respectively, using a red outline. They represent 33% and 59%, respectively, of the measured eyes for the horizontal and vertical components.

The absolute distance between the AcP and PI is also relevant. Figure 5 shows the location of the AcP relative to that of PI for each eye. A red outline highlights those eyes for which this distance is statistically significant. Although for most measured eyes both points are not coincident, on average they were for the studied set of eyes. The mean location of the AcP relative to that of the PI was [$x = -0.05 \pm 0.15$ mm; $y = 0.09 \pm 0.18$ mm], where the error was ± 1 standard deviation. Moreover, the histogram of distances represented in Figure 5 revealed that for approximately half of the eyes (55%), the distance between locations was less than 0.2 mm and was less than 0.4 mm in 95% of the cases. We did not find any eye where the AcP was separated by more than 0.6 mm from PI. For the sake of clarity, we omitted error bars in Figures 3 through 5. Figure 6 shows the histogram of the distance between the achromatic pupil (AcP) and PI.

DISCUSSION

We designed and implemented a new instrument to simultaneously determine the position of both the achromatic axis intersection with the pupil (AcP) and the first Purkinje image (PI) reflection in a normal population. The distance between these two marks on the pupil plane is relevant to better understand the suitability of the current centration procedures in corneal refractive surgery. It is common to use PI as the reference point assuming that it is close to the intersection of the achromatic axis with the pupil (AcP). Our results showed that on average, the location of both marks were coincident within our measurement error. This somehow validated the current surgical practice; however, an individual analysis reflects some issues to be considered.

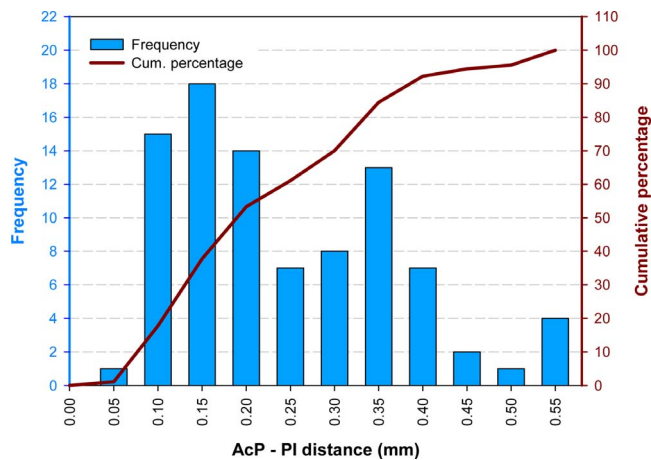


FIGURE 6. Histogram of the distances between the AcP and PI.

We found that 28% of the measured eyes presented no statistically significant distances between these two points, another 27% of eyes showed a statistically significant distance but it was less than 0.2 mm, and only in 5% of the cases was the distance greater than 0.4 mm. According to a previous study,¹⁴ 0.4 mm can be considered as a limiting value for the permissible distance between PI and AcP. Use of the PI as the reference point in corneal surgical procedures might compromise the quality of vision in those eyes where the distance between PI and AcP is larger than 0.4 mm (5% in our sample). On the other hand, according to Figure 3, AcP is on average slightly closer than the PI to the pupil's center along the horizontal direction. The slope (0.79) of the linear fitting is smaller than 1 and, indeed the proportion of eyes where the AcP lay somewhere between the pupil center and the PI (being not coincident) was 82%. Hence, on average, our results support the currently used centration procedures on the PI or close to it, along the direction to the pupil center. However, the results shown in Figure 5 suggest that the nasal-inferior quadrant relative to the PI should be avoided because we did not find any eye with its AcP located in this area.

Although our results suggest that they represent a small fraction of the population, it would be interesting for the surgeon to be able to identify in advance those subjects whose PI and AcP are separated by more than 0.4–0.5 mm). In an attempt to find a possible screening technique, we tried a number of statistical correlations between AcP-to-PI distances and different biometric parameters measured in the same group of eyes. We did not find any correlation between the marks' distances and axial length, age, refraction, or pupil diameter.

In a further attempt to clarify the origin of our results, we performed customized ray-tracing simulations. By using a previously established procedure,¹⁹ we built a set of 20 eye models from actual data measured in 20 young subjects: corneal topography, anterior chamber depth, axial length, angle kappa, and ocular spherical aberration. The refractive indices of the optical media were taken from published data.²⁰ Initially, all optical surfaces of the eye were centered along an optical axis, and the only misalignment included was the angle kappa. In this situation, the position of the achromatic axis, calculated as the pupil position producing overlapped retinal images for blue (400 nm) and red (600 nm) rays, and the position of the corneal reflection over the pupil plane perfectly matched each other ($R^2 = 0.999$). This simulation further validated the choice of the corneal reflection as the reference for the implantation of corneal inlays. However, it does not

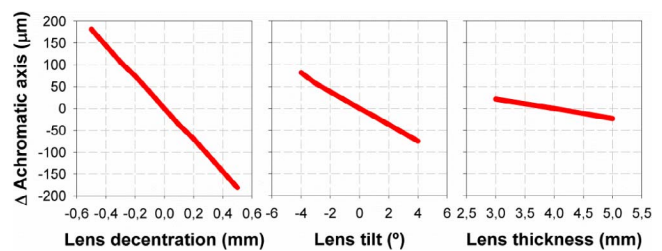


FIGURE 7. Changes in the position of the achromatic axis intersection with the pupil plane (AcP) as a function of lens decentration, lens tilt, and lens thickness.

explain the experimental variability observed in the distance between PI and AcP.

In a second series of ray-tracing simulations, we explored the effects of lens decentration, lens tilt, and lens thickness on the AcP position. Three of the previous model eyes were randomly chosen, and the achromatic pupil position was calculated as a function of these three parameters. The range of induced lens decentration was ± 0.5 mm; lens tilt was changed within a range of $\pm 4^\circ$; and lens thickness was increased up to 2 mm over the initial value. The average results of these simulations are presented in Figure 7. Linear addition of these three factors can account for distances between PI and AcP in the range of ± 0.325 mm, and 79% of our population was in this range. Larger distances might be explained by additional factors like larger misalignments, nonlinear additive effects, or chromatic effects of the gradient index distribution of the crystalline lens (not considered in the simulations).

The results and conclusions reported in this paper are based on measurements performed in a population composed mainly of young individuals with moderate refractive errors. Whether conclusions may be extrapolated to different ranges of age and refractive error requires further investigation, but it is worth noting that in our sample, no correlation was found with any of these features.

Although pupils may change centration with dilation, this did not affect our results, because we used the pupil center simply as a reference to estimate the positions of the used marks.

In conclusion, we designed and built an instrument to simultaneously measure the position of the corneal reflex and the achromatizing pupil position. We measured these features in a population of 90 eyes, finding that these two points virtually overlap on average and that individually they are closer than 0.4 mm in 95% of eyes. This result supports the use of the corneal reflex as an estimate of the achromatic axis position, which currently is one of the most widely used targets for corneal surgery. However, when possible, it is recommended that screening for patients showing discrepancies between these two marks that can severely impact the optical and visual outcomes of the surgical procedures.

Acknowledgments

Preliminary parts of this research were presented at the annual meeting of the Association for Research in Vision and Ophthalmology, Seattle, Washington, United States, May 2013 (Manzanera, et al. *IOVS* 2013;54:ARVO E-Abstract 4281).

This research was supported by European Research Council Advanced Grant ERC-2013-AdG-339228 (SEECAT) and Spanish SEIDI Grant FIS2013-41237-R.

Disclosure: **S. Manzanera**, None; **P.M. Prieto**, None; **A. Benito**, None; **J. Tabernero**, None; **P. Artal**, None

References

- Pallikaris IG, Siganos DS. Excimer laser in-situ keratomileusis and photorefractive keratectomy for correction of high myopia. *J Refract Corneal Surg.* 1994;10:498-510.
- Ditzen K, Huschka H, Pieger S. Laser in situ keratomileusis for hyperopia. *J Cataract Refract Surg.* 1998;24:42-47.
- Kriegerowski M, Bende T, Seiler T, Wollensak J. The ablation behavior of various corneal layers. *Fortschr Ophthalmol.* 1990;87:11-13.
- Miller D, Blanco E, inventors; Boston Innovative Optics, Inc., assignee. System and method for increasing the depth of focus of the human eye. US patent 6874886. April 5, 2008.
- Uozato H, Guyton DL. Centering corneal surgical procedures. *Am J Ophthalmol.* 1987;103:264-275.
- Pande M, Hillman JS. Optical zone centration in keratorefractive surgery. Entrance pupil center, visual axis, coaxially sighted cornea reflex or geometrical corneal center? *Ophthalmology.* 1993;100:1230-1237.
- Chan CCK, Wachler BSB. Centration analysis of ablation over the coaxial corneal light reflex for hyperopic LASIK. *J Refract Surg.* 2006;22:467-471.
- de Ortueta D, Schreyer FD. Centration on the cornea vertex normal during hyperopic refractive photoablation using videokeratoscopy. *J Refract Surg.* 2007;23:198-200.
- Soler V, Benito A, Soler P, et al. Randomized comparison of pupil-centered versus vertex-centered ablation in LASIK correction of hyperopia. *Am J Ophthalmol.* 2011;152:591-599.
- Tabernero J, Schwarz C, Fernandez EJ, Artal P. Binocular visual simulation of a corneal inlay to increase depth of focus. *Invest Ophthalmol Vis Sci.* 2011;52:5273-5277.
- Ivanoff A. Sur une methode de mesure des aberrations chromatiques et spheriques de l'oeil en lumiere dirige. *Comptes Rendu Academie Science.* 1946;170-172.
- Thibos LN, Bradley A, Still DL, Zhang X, Howarth PA. Theory and measurement of ocular chromatic aberration. *Vis Res.* 1990;30:33-49.
- Artal P, Marcos S, Iglesias I, Green DG. Optical modulation transfer and contrast sensitivity with decentered pupils in the human eye. *Vis Res.* 1996;36:3575-3586.
- Tabernero J, Artal P. Optical modeling of a corneal inlay in real eyes to increase depth of focus: optimum centration and residual defocus. *J Cataract Refract Surg.* 2012;38:270-277.
- Yilmaz OE, Bayraktar S, Agca A, Yilmaz B, McDonald MB, van de Pol C. Intracorneal inlay for the surgical correction of presbyopia. *J Cataract Refract Surg.* 2008;34:1921-1927.
- Seyeddain O, Riha W, Hohensinn M, Nix G, Dextl AK, Grabner G. Refractive surgical correction of presbyopia with the AcuFocus small aperture corneal inlay: two-year follow-up. *J Refract Surg.* 2010;26:707-715.
- Gatinel D, El Danasoury A, Rajchles S, Saad A. Recentration of a small-aperture corneal inlay. *J Cataract Refract Surg.* 2012; 38:2186-2191.
- Rynders M, Lidkea B, Chisholm W, Thibos LN. Statistical distribution of foveal transverse chromatic aberration, pupil centration, and angle-psi in a population of young-adult eyes. *Vision Res.* 1995;12:2348-2357.
- Tabernero J, Benito A, Alcon E, Artal P. Mechanism of compensation of aberrations in the human eye. *J Opt Soc Am A Opt Image Sci Vis.* 2007;24:3274-3283.
- Navarro R, Santamaria J, Bescos J. Accommodation-dependent model of the human-eye with aspherics. *Vision Res.* 1985;2: 1273-1281.